Available online at www.sciencedirect.com
SCIENCE DIRECT®
ELSEVIER
International Communications in Heat and Mass Transfer 33 (2006) 135–141
International Communications in HEAT and MASS TRANSFER
www.elsevier.com/locate/ichmt

Cooling effect of thermally significant blood vessels in perfused tumor tissue during thermal therapy ☆

Tzu-Ching Shih [a,*], Hao-Li Liu [b], Allen Tzyy-Leng Horng [c]

[a] *Department of Medical Radiology Technology, China Medical University, Taiwan*
[b] *Department of Electrical Engineering, Chang Gung University, Taiwan*
[c] *Department of Applied Mathematics, Feng Chia University, Taiwan*

Available online 13 September 2005

Abstract

This purpose of this article was focused on the cooling effects of thermally significant blood vessels on the extent of thermal lesion during heating treatments. The thermal modeling here based on the Pennes bio-heat transfer equation, describing the heat transfer of perfused tumor tissue, and the energy transport equation governing the heat convection and diffusion of the blood flow. The explicit finite difference method was used to solve the transient equation for the temperature field of a perfused tumor tissue encompassing a blood vessel in an axis-symmetric configuration during thermal therapy. As a result of simulation, the short-duration high-intensity heating is more effective on covering the treated tumor inside with a blood vessel 200 μm in diameter. For a blood vessel inside tumor tissue with a diameter larger than 2 mm, it is observed that neither longer heating duration nor higher heating power density is sufficient for complete necrosis of tumor.

Keywords: Thermally significant blood vessel; Bio-heat transfer equation; Thermal therapy

1. Introduction

Tumor cells with a distance of more than 100 μm from the capillary were regarded as hypoxic cells, viable but unable to divide so that the blood vessels are essential to tumor growth and metastasis [1]. The thermally significant blood vessels (larger than 200 μm in diameter) can affect the temperature distribution in heated tissue during thermal therapy [2–4]. The time evolution of temperature field in tissue modeled by famous Pennes' bio-heat transfer equation neglects the local cooling effect of large blood vessel (i.e., the thermally significant blood vessel) inside the tissue [5]. Furthermore, Craciunescu and Clegg discussed the effects of pulsating blood flow on the temperature distribution of heated tissue [6]. They found that the pulsation of blood flow rate yields an obvious change of the energy transport between the vessel wall and the blood flow within large blood vessel based on the assumption that the vessel wall is a perfect thermal sink (i.e. the temperature of the wall is a constant). However, they only focused on heat transfer between the blood flow and the vessel wall, not considering heat exchange between the living tissue and blood vessel in whole. Moreover, Gowrishankar et al.

☆ Communicated by W.J. Minkowycz.
* Corresponding author.
E-mail address: shih@mail.cmu.edu.tw (T.-C. Shih).

0735-1933/$ - see front matter © 2005 Elsevier Ltd. All rights reserved.
doi:10.1016/j.icheatmasstransfer.2005.08.003

separated heat transport processes by using a lattice that employs the Pennes' bio-heat equation in perfused tissues, and pure diffusion in non-perfused regions [7]. They used this lattice approach to model heat transfer by conduction and temperature-dependent blood perfusion separately through a network model accounting for locally interacting transport, storage and source, and further solved the resultant system by Kirchhoff's law. However, their lattice model can only be applied to heat transport in skin with spatially heterogeneous, temperature-dependent perfusion, which is not suitable to extend to the heat transfer problem of thermally significant blood vessels inside a tumor.

In addition, Cheng and Roemer, neglecting blood perfusion effects, showed the minimum treatment time for a single heat pulse delivered to the heating target with a closed-form thermal dose solution [8]. They found that the total treatment time decreases as the size of the applied power zone increases for multiple-pulse thermal treatment. However, they did not consider the influence of blood flow of thermally significant blood vessel either. Therefore, this article is motivated to investigate the cooling effect of thermally significant blood vessels on the extent of thermal lesion during thermal treatment.

2. Mathematical model and numerical method

2.1. Governing equations and numerical method

Here we consider a single blood vessel inside and throughout the perfused tumor tissue in a three-dimensional axis-symmetric geometric configuration as shown in Fig. 1. The energy transport equations of tissue and blood are represented in Eqs. (1) and (2), respectively.

$$\rho_t c_t \frac{\partial T}{\partial t} = k_t \left[\frac{1}{r} \frac{\partial}{\partial r} \left(r \frac{\partial T}{\partial r} \right) + \frac{\partial^2 T}{\partial z^2} \right] - W_b c_b (T - T_a) + Q_t(r,z,t), \tag{1}$$

$$\rho_b c_b \left(\frac{\partial T}{\partial t} + w \frac{\partial T}{\partial z} \right) = k_b \left[\frac{1}{r} \frac{\partial}{\partial r} \left(r \frac{\partial T}{\partial r} \right) + \frac{\partial^2 T}{\partial z^2} \right] + Q_b(r,z,t). \tag{2}$$

The diameters of thermally significant blood vessel and the associated blood flow velocities are presented in Table 1. The wall of the blood vessel is considered rigid here for simplicity. The tissue temperature outside the thermally significant blood vessel is modeled by Pennes' bio-heat transfer equation in cylindrical coordinates as shown in Eq. (1). The perfusion term in Eq. (1) describes the heat sink of the microvascular blood flow during heating treatments. The temperature of the blood flow is governed by Eq. (2).

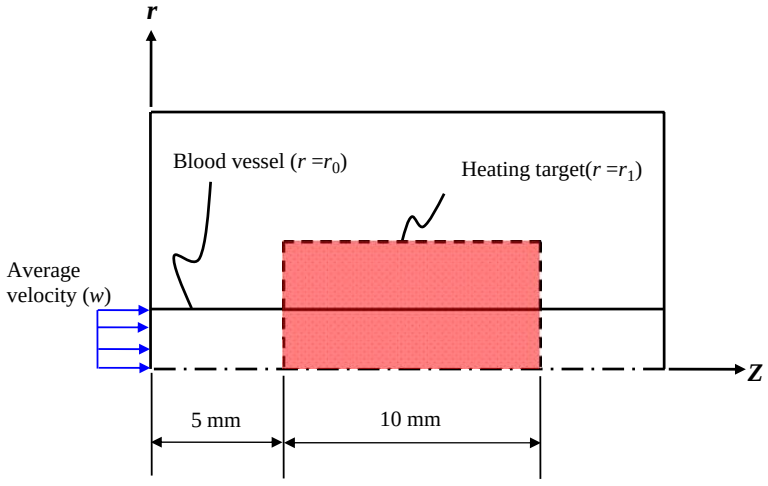

Fig. 1. The heating target volume is specified as 5 mm $\leqq z \leqq$ 15 mm and $0 \leqq r \leqq$ 5 mm, and the velocity profile in the blood vessel is assumed to be uniform. Various diameters ($2r_0$) of the blood vessels are shown in Table 1.

Table 1
Blood vessel characteristics of a 13-kg dog after reference [3,13]

Diameter (mm)	Blood velocity in normal tissue (mm/s)	Average blood velocity in tumor (w) (mm/s)
0.2	34	3.4
0.6	60	6
1.0	80	8
1.4	60	10.5
2.0	200	20

To nondimensionalize Eqs. (1) and (2), several dimensionless parameters are defined as follows:

$$\theta = \frac{T - T_a}{T_a}, \quad R = \frac{r}{r_0}, \quad Z = \frac{z}{r_0}, \quad \tau = \frac{k_t t}{\rho_t c_t r_0^2}. \tag{3}$$

We can then rewrite Eqs. (1) and (2) into one formula with the different values of coefficients for blood vessel and tumor tissue

$$\frac{\partial \theta}{\partial \tau} + A_1 \frac{\partial \theta}{\partial Z} = \frac{1}{R}\frac{\partial}{\partial R}\left(R\frac{\partial \theta}{\partial R}\right) + \frac{\partial^2 \theta}{\partial Z^2} - A_2\theta + A_3, \tag{4}$$

where

$$A_1 = \frac{\rho_t c_t w r_0}{k_t}, \quad A_2 = \frac{W_b c_b r_0^2}{k_t}, \quad A_3 = \frac{r_0^2 Q}{k_t T_a}.$$

It is noticeable here that the term A_1 equals zero for the tissue domain, and the term A_2 becomes zero for the blood vessel domain.

Here, we used time-explicit finite difference method to discretize Eq. (4) into

$$\theta_{i,j}^{n+1} = c_1\theta_{i,j}^n + c_2\theta_{i+1,j}^n + c_3\theta_{i-1,j}^n + c_4\theta_{i,j+1}^n + c_5\theta_{i,j-1}^n + c_6, \tag{5}$$

where

$$c_1 = 1 - c_2 - c_3 - c_4 - c_5 - A_2\Delta\tau,$$

$$c_2 = \frac{\Delta\tau}{(\Delta Z_i)(\Delta Z_{i+1/2})},$$

$$c_3 = A_1\frac{\Delta\tau}{\Delta Z_i} + \frac{\Delta\tau}{(\Delta Z_i)(\Delta Z_{i-1/2})},$$

$$c_4 = \frac{(R_{j+1/2})\Delta\tau}{(R_j)(\Delta R_j)(\Delta R_{j+1/2})},$$

$$c_5 = \frac{(R_{j-1/2})\Delta\tau}{(R_j)(\Delta R_j)(\Delta R_{j-1/2})},$$

$$c_6 = A_3\Delta\tau.$$

Then we solved Eq. (5) for the time evolution of temperature for both tissue and blood vessel. Usually the blood vessel in tumors has a smaller flow rate than in the host's normal tissues. Hence the average blood flow velocity in blood vessel of tumor is set to be 0.1 times that in normal tissue [9]. In the current simulation, the heat power is deposited by ultrasound, and the heat absorption rate of blood is about 1/10 of tissue [10].

Table 2
Parameters of the three heating schemes used in numerical simulations

	Case								
	I	II	III	IV	V	VI	VII	VIII	IX
Heating power density (W/cm^3)	60	12	4	60	12	4	120	24	8
Heating duration (s)	2	10	30	4	20	60	2	10	30

2.2. Thermal dose calculation

The accumulated thermal dose in tissue is function of the heating duration and the temperature level. The thermal dose or equivalent minutes at 43 °C (EM_{43}) is defined by Sapareto and Dewey [11]:

$$EM_{43}(\text{in min}) = \int R^{(T-43)} dt, \tag{6}$$

where $R=2$ for $T \geq 43$ °C, $R=4$ for 37 °C $< T <$ 43 °C, T is temperature, and t is time. The threshold dose for necrosis is $EM_{43}=240$ min for muscle tissue [12]. Therefore this conservative value 240 min (EM_{43}) is taken for thermal damage to tumor tissue in this study. Parameters characterizing nine different heating schemes were depicted in Table 2.

3. Results and discussion

The effect of increasing heating duration and at the same time decreasing heating power density while the absorbed total energy density is kept constant as 120 J/cm^3 corresponding to heating schemes I–III in Table 2 for blood vessel of diameter 0.2 mm and average blood flow velocity 3.4 mm/s (see Fig. 2(a)–(c)). The cooling effect of blood vessels is more obvious for longer heating (case III). It means that short-duration high-intensity heating covers the treated tumor more effectively for such a blood vessel. In

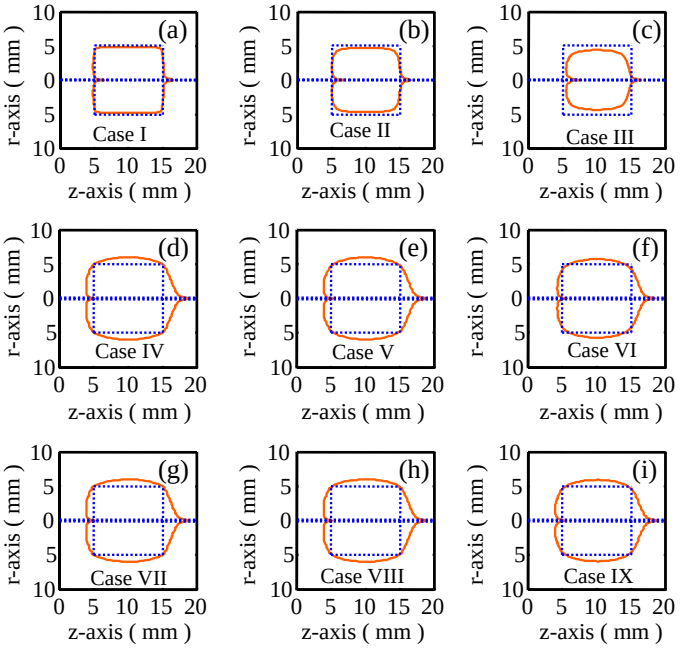

Fig. 2. Effect of the heating schemes (I–IX) on the thermal dose contours $EM_{43}=240$ min at $t=90$ s for the blood vessel 200 μm in diameter. The blood vessel boundaries are denoted with the horizontal dashed lines, and the heated target region is denoted a square with the dashed lines. Here $r_0=0.1$ mm, $w=3.4$ mm/s, $r_1=5$ mm, $W_b=0.5$ kg/m^3 s, $k_b=k_t=0.5$ W/m °C.

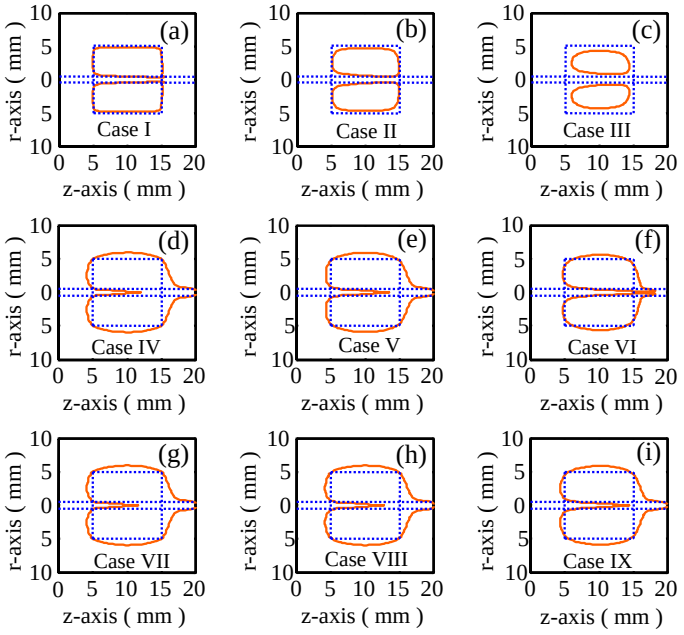

Fig. 3. Effect of the heating schemes (I–IX) on the thermal dose contours $EM_{43}=240$ min at $t=90$ s for the blood vessel 1 mm in diameter. The blood vessel boundaries are denoted with the horizontal dashed lines. The heated target region is denoted a square with the dashed lines. Here $r_0=0.5$ mm, $w=8$ mm/s, $r_1=1$ mm, $W_b=0.5$ kg/m^3 s, $k_b=k_t=0.5$ W/m °C.

Fig. 2(d)–(i), it is clearly that the cooling effect of blood vessel is indifferent to heating schemes when the total absorbed energy density is doubled as before, corresponding to the cases IV–IX in Table 2.

In Fig. 3, the cooling effect of a blood vessel 1 mm in diameter and the average blood flow velocity 8 mm/s on the thermal dose contours $EM_{43}=240$ min are presented. Taking Fig. 3(a) (case I) as an example, a heating power density 60 W/

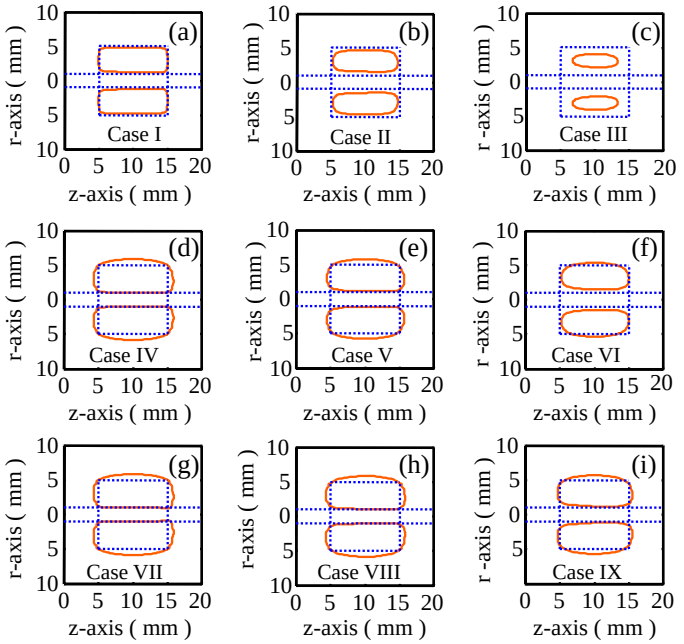

Fig. 4. Effect of the heating schemes (I–IX) on the thermal dose contours $EM_{43}=240$ min at $t=90$ s for the blood vessel 2 mm in diameter. The blood vessel boundaries are denoted with the horizontal dashed lines. The heated target region is denoted a square with the dashed lines. Here $r_0=1$ mm, $w=20$ mm/s, $r_1=1$ mm, $W_b=0.5$ kg/m^3 s, $k_b=k_t=0.5$ W/m °C.

cm^3 is applied for 2 s and it turned out sufficient to produce the thermal lesion region for tumor tissue immediately adjacent to the blood vessel. However the vessel itself did not achieve complete necrosis. Even when larger energy is applied, such as 2nd and 3rd rows in Fig. 3, part of blood vessel still did not achieve complete necrosis, and the targeted thermal lesion region in tissue was enlarged. In order to completely cover the heated volume, the heating pattern obviously needs to be improved.

This cooling effect becomes stronger when both the diameter and flow velocity of blood vessel are larger such as cases in Fig. 4 with vessel diameter 2 mm and average flow velocity 20 mm/s. In Fig. 4(b) and (c), the thermal lesion still cannot cover the whole tissue surrounding the blood vessel. In Fig. 4(g) (case VII), the accumulated thermal dose in some part of blood vessel was observed to be far less than 1 min (EM_{43}). In addition, the targeted thermal lesion region in tissue was enlarged in 2nd and 3rd rows of Fig. 4.

4. Conclusions

The short-duration and high-intensity heating scheme can completely reduce the cooling effect of the blood vessel 200 μm in diameter. For larger blood vessels, however, the cooling effect is stronger, and the thermal lesion of targeted volume is not sufficient to achieve complete necrosis even using a double heating duration or heating power density. In addition, even inputting more energy into the heated target volume, the cooling effect of the thermally significant blood vessel is still strong and then may cause a pronounced overheating of the surrounding normal tissue especially near the downstream of blood vessel.

Nomenclature

c	specific heat (J/kg °C)
k	thermal conductivity (W/m °C)
t	time (s)
T	temperature (°C)
T_a	arterial temperature = 37(°C)
θ	nondimensional temperature $\theta = ((T - T_a)/T_a)$
Q	absorbed power deposition density (W/cm^3)
w	average blood velocity along z-directional (mm/s)
r	distance along r-axis (mm)
r_0	radius of the blood vessel
r_1	radius of the heating tumor tissue
z	distance along z-axis (mm)
R	nondimensional $R = r/r_0$
Z	nondimensional $Z = z/r_0$
W_b	blood perfusion rate (kg/m^3 s)
ρ	density (kg/m^3)
τ	nondimensional time $\tau = (k_t t/\rho_t c_t r_0^2)$

Subscripts

b	blood
t	tissue

Acknowledgments

I would like to thank Win-Li Lin for his many helpful comments and suggestions that greatly improved this paper.

References

[1] M. Kocher, H. Treuer, J. Voges, M. Hoevels, V. Sturm, R. Muller, Computer simulation of cytotoxic and vascular effects of radiosurgery in solid and necrotic brain metastases, Radiother. Oncol. 54 (2) (2000) 149–156.

[2] J. Crezee, J.J.W. Lagendijk, Experimental verification of bioheat transfer theories: measurement of temperature profiles around large artificial vessels in perfused tissue, Phys. Med. Biol. 35 (7) (1990) 905–923.

[3] M.C. Kolios, M.D. Sherar, J.W. Hunt, Blood flow cooling and ultrasonic lesion formation, Med. Phys. 23 (7) (1996) 1287–1298.
[4] T.C. Shih, H.S. Kou, W.L. Lin, Effect of effective tissue conductivity on thermal dose distributions of living tissue with directional blood flow during thermal therapy, Int. Commun. Heat Mass Transf. 30 (1) (2002) 115–126.
[5] H.H. Pennes, Analysis of tissue and arterial blood temperature in the resting human forearm, J. Appl. Physiol. 1 (2) (1948) 93–122.
[6] O.I. Craciunescu, S.T. Clegg, Pulsatile blood flow effects on temperature distribution and heat transfer in rigid vessels, ASME J. Biomech. Eng. 123 (5) (2001) 500–505.
[7] T.R. Gowrishankar, D.A. Stewart, G.T. Martin, J.C. Weaver, Transport lattice models transport in skin with spatially heterogeneous, temperature-dependent perfusion, Biomed. Eng. Online 3 (42) (2004) 1–17.
[8] K.S. Cheng, R.B. Roemer, Blood perfusion and thermal conduction effects in Gaussian beam, minimum time single-pulse thermal therapies, Med. Phys. 32 (2) (2005) 311–317.
[9] C.W. Song, I.B. Choi, B.S. Nah, S.K. Sahu, J.L. Osborn, Thermoradiotherapy and Thermochemotherapy, Biology, Physics, Physics, vol. 1, Springer-Verlag, Berlin, 1995, p. 139.
[10] F.A. Duck, Physical Properties of Tissues: A Comprehensive Reference Book, Academic Press, San Diego, 1990.
[11] S.A. Sapareto, W. Dewey, Thermal dose determination in cancer therapy, Int. J. Radiat. Oncol. Biol. Phys. 10 (6) (1984) 787–800.
[12] C. Damianou, K. Hynynen, Focal spacing and near-field heating during pulsed high temperature ultrasound therapy, Ultrasound Med. Biol. 19 (9) (1993) 777–787.
[13] J.C. Chato, Heat transfer to blood vessels, ASME J. Biomech. Eng. 102 (2) (1980) 110–118.